ACS OMEGA

http://pubs.acs.org/journal/acsodf

Article

Dimeric Diarylheptanoids with Neuroprotective Activities from Rhizomes of *Alpinia officinarum*

Hui Liu,[⊥] Xiaojun Wang,[⊥] Qiaoyun Shi,[⊥] Liuren Li, Qinghua Zhang, Zhen-Long Wu, Xiao-Jun Huang, Qing-Wen Zhang, Wen-Cai Ye, Ying Wang,* and Lei Shi*

Cite This: *ACS Omega* 2020, 5, 10167−10175

Read Online

ACCESS | Metrics & More | Article Recommendations | Supporting Information

ABSTRACT: Two novel dimeric diarylheptanoids, alpinidinoids A [(±)-**1**] and B (**2**), with two unusual coupling patterns, together with a new naturally occurring diarylheptanoid dimer possessing a rare pyridine ring linkage (alpinidinoid C, **3**), were isolated from the rhizomes of *Alpinia officinarum*. Their structures including absolute configurations were determined by extensive spectroscopic methods and theoretical calculations. All isolates were examined for their neuroprotective activities against oxygen-glucose deprivation and reoxygenation (OGD/R) damage in primary cortical neurons. Remarkably, the dextrorotatory enantiomer of alpinidinoid A [(+)-**1**] significantly ameliorated OGD/R-induced neuronal apoptosis, which was dependent on the activation of the AKT/mTOR signaling pathway.

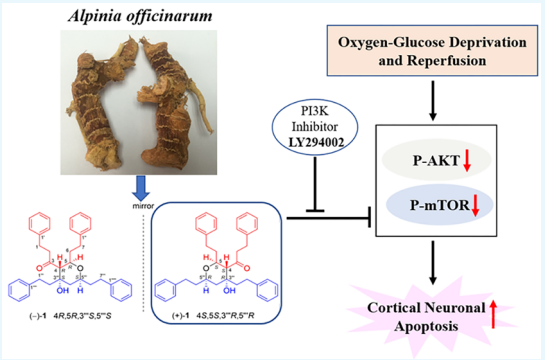

INTRODUCTION

Brain ischemia is a very common cause of mortality and disability worldwide, which generally occurs due to the critical reduction of brain blood supply.[1,2] The major manifestation of brain ischemia is ischemic stroke, ranking the second cause of death globally. It is estimated that 17 000 000 people suffer from a stroke each year and about 80% of these conditions are caused by cerebral ischemia.[3,4] Reperfusion to ischemic brains is an approach to reverse brain damage. Nonetheless, reperfusion also leads to secondary tissue damage accompanied by death and dysfunction of brain cells, called ischemia/reperfusion (I/R) injury.[5,6] Multiple studies indicate that apoptosis is a major form of cell death after cerebral I/R, and the prosurvival AKT/mTOR signaling pathway is inhibited during neuronal apoptosis.[7−9] Thus, the activators of the AKT/mTOR pathway could be potential therapeutic agents for brain ischemia.

As reported in numerous reports, natural products derived from food exhibit significant effects on the treatment of cerebral ischemic injury, revealing a potent resource of neuroprotective agents.[10−12] The plant *Alpinia officinarum* Hance, belonging to family Zingiberaceae, is an important edible medicinal plant widely cultivated in the tropical and subtropical areas of Asia.[13] The rhizomes of *A. officinarum*, commonly known as lesser galangal, are not only widely utilized as an important food spice and flavoring agent but also used as a traditional Chinese medicine in China for the treatment of gastrointestinal diseases.[14,15] Phytochemical investigations have revealed that diarylheptanoids are the characteristic constituents of the rhizomes of *A. officinarum*, which exhibit a variety of biological activities, such as antioxidant,[16] antibacterial,[17] anticancer,[18] antiemetic,[19] and anti-inflammatory activities.[20] As a result of our continuing efforts to discover natural products with nervous system activities, our previous studies on the title plant had resulted in the discovery of a series of diarylheptanoids with promising neuroprotective effects, including promoting neuronal differentiation and neurite outgrowth, against Aβ-induced damage and against 1-methyl-4-phenylpyridinium (MPP^+)-induced injury in neuronal cells or primary cortical neurons.[21−24] Recently, we also found that 7-(4-hydroxy-3-methoxyphenyl)-1-phenyl-4*E*-hepten-3-one protects cortical neurons against oxygen-glucose deprivation and reoxygenation (OGD/R) injuries.[25] In the current study, a pair of new dimeric diarylheptanoid enantiomers [(±)-alpinidinoid A, (±)-**1**], a new axisymmetrical diarylheptanoid dimer (alpinidinoid B, **2**), and a new naturally occurring dimeric diarylheptanoid with a rare pyridine ring linkage (alpinidinoid C, **3**) were isolated from the nonpolar fraction of *A. officinarum* (Figure 1). Notably, the two monomeric diarylheptanoid motifs in **1** were connected through the C-4−C-3‴ and C-5−*O*−C-5‴ bonds to form a tetrahydropyran ring, which is unprecedented in dimeric diarylheptanoids. In **2**, the two monomeric diary-

Received: March 6, 2020
Accepted: April 9, 2020
Published: April 22, 2020

https://dx.doi.org/10.1021/acsomega.0c01019
ACS Omega 2020, 5, 10167−10175

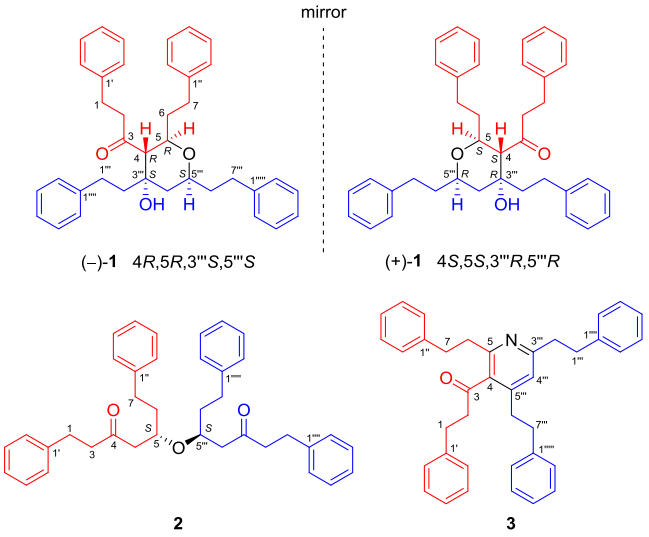

Figure 1. Chemical structures of **1**−**3** from the rhizomes of *A. officinarum*.

lheptanoid units were bridged via an oxygen atom through C-5−*O*−C-5‴ bonds and thereby constructed a novel symmetrical scaffold with a C_2 symmetry axis. The neuroprotective activities of all compounds against OGD/R damage in primary cortical neurons were evaluated. The results showed that (+)-**1** significantly ameliorated OGD/R-induced neuronal apoptosis. Further mechanism investigations revealed that the activation of the AKT/mTOR signaling pathway was involved in the neuroprotective effect of (+)-**1**. Herein, we describe the isolation, structural elucidation, and the neuroprotective activities of these diarylheptanoid dimers.

RESULTS AND DISCUSSION

Alpinidinoid A (**1**) was isolated as a yellow oil. The molecular formula of **1** was determined as $C_{38}H_{42}O_3$ by its HR-ESI-MS data (*m*/*z* 545.3055 $[M - H]^-$, calcd for $C_{38}H_{41}O_3$: 545.3056), indicating 18 degrees of unsaturation in its molecule. The UV spectrum revealed the absorption bands at λ_{max} 208 and 262 nm. The IR spectrum indicated the presence of hydroxy (3448 cm^{-1}), carbonyl (1687 cm^{-1}), and aromatic ring (1601 and 1493 cm^{-1}) functional groups in **1**. Analysis of ^1H and ^{13}C NMR spectral data (Table 1) revealed the presence of a ketone carbonyl (δ_C 215.9), four monosubstituted benzene rings [δ_H 7.08−7.12 (6H, overlapped), 7.13−7.16 (1H), 7.17−7.21 (7H, overlapped), and 7.25−7.30 (6H, overlapped); δ_C 142.1, 141.9, 141.6, 140.3, 128.5 × 2, 128.46 × 2, 128.44 × 4, 128.4 × 4, 128.36 × 2, 128.3 × 2, 126.3, 125.90, 125.87, and 125.8], three methines [δ_H 3.86 (1H, m), 3.81 (1H, td, *J* = 9.8, 2.3 Hz), and 2.65 (1H, d, *J* = 9.8 Hz); δ_C 74.1, 72.0, and 61.5], an oxygenated quaternary carbon (δ_C 72.3), and nine alkyl methylene groups.

Interpretation of the $^1H-^1H$ COSY spectrum of **1** elucidated eight spin-coupling systems in **1** (Figure 2). Besides, the heteronuclear multiple bond correlation (HMBC) cross-peaks between H_2-1 and C-3/C-2′ (C-6′), between H_2-2 and C-1′, between H-4 and C-2, between H_2-6 and C-1″, and between H_2-7 and C-2″ (C-6″) allowed the construction of a diarylheptanoid motif **1a**. Meanwhile, the HMBC correlations between H_2-1‴ and C-3‴/C-2‴′ (C-6‴′), between H_2-2‴ and C-1‴′/C-4‴, between H_2-6‴ and C-1‴″, and between H_2-7‴ and C-2‴″ (C-6‴″) led to the establishment of another

Table 1. ^1H and ^{13}C NMR Spectroscopic Data for 1 and 3 (δ in ppm, *J* in Hz)[a]

	1[b]		3[c]	
no.	δ_C	δ_H	δ_C	δ_H
1	28.5	2.83	29.8	2.95 (t, 7.0)
2	49.7	2.85	47.4	2.85
3	215.9		208.0	
4	61.5	2.65 (d, 9.8)	135.8	
5	74.1	3.81 (td, 9.8, 2.3)	155.6	
6	36.3	a: 1.69	38.3	2.81
		b: 1.37 (m)		
7	31.8	a: 2.90 (m)	36.2	3.03
		b: 2.62 (m)		
1′	140.3		141.9[d]	
2′, 6′	128.4[d]	7.08−7.12	129.34[d]	7.20−7.30
3′, 5′	128.5[d]	7.17−7.21	129.5[d]	7.20−7.30
4′	125.87[d]	7.13−7.16	126.9[d]	7.14−7.19
1″	141.6[d]		141.9[d]	
2″, 6″	128.4[d]	7.17−7.21	129.2[d]	7.20−7.30
3″, 5″	128.46[d]	7.25−7.30	129.27[d]	7.20−7.30
4″	126.3[d]	7.17−7.21	126.68[d]	7.14−7.19
1‴	29.3[d]	a: 2.72	36.0	3.04
		b: 2.58		
2‴	44.4	1.58 (m)	40.4	3.05
3‴	72.3		161.4	
4‴	40.6	*α*: 1.78 (dd, 13.5, 2.1)	121.8	6.97 (br s)
		β: 1.22 (dd, 13.5, 11.2)		
5‴	72.0	3.86 (m)	147.2	
6‴	37.6	a 1.85	35.3	2.64 (m)
		b 1.71		
7‴	32.0	a 2.92	37.4	2.79
		b 2.72		
1‴′	142.1[d]		142.7[d]	
2‴′, 6‴′	128.44[d]	7.08−7.12	129.1[d]	7.06−7.11
3‴′, 5‴′	128.44[d]	7.25−7.30	129.34[d]	7.20−7.30
4‴′	125.90[d]	7.17−7.21	126.69[d]	7.14−7.19
1‴″	141.9[d]		141.9[d]	
2‴″, 6‴″	128.36[d]	7.08−7.12	129.1[d]	7.06−7.11
3‴″, 5‴″	128.3[d]	7.25−7.30	129.34[d]	7.20−7.30
4‴″	125.8[d]	7.17−7.21	126.8[d]	7.14−7.19

[a]Overlapped resonances are reported without designating multiplicity. [b]Measured in $CDCl_3$. [c]Measured in acetone-d_6. [d]Interchangeable assignments.

diarylheptanoid moiety **1b**. Furthermore, the HMBC cross-peaks between H_2-2‴/H_2-4‴ and C-4 and between H-5 and C-5‴, together with the molecular formula information and the obvious down-field shifts of C-5 (δ_C 74.1) and C-5‴ (δ_C 72.0), indicated that substructures **1a** and **1b** were connected via the C-4−C-3‴ bond and the oxygen bridge between C-5 and C-5‴ to form a tetrahydropyran ring (Figure 2).

The relative configuration of the partial structure of **1** could be deduced on the basis of the coupling constant of vicinal protons and the nuclear Overhauser enhancement spectroscopy (NOESY) spectrum. The large coupling constants of $^3J_{H\text{-}4,H\text{-}5}$ (9.8 Hz) and $^3J_{H\text{-}4'''\beta,H\text{-}5'''}$ (11.2 Hz) indicated that H-4 and H-5 as well as H-4‴*β* and H-5‴ were trans-related, respectively. In the NOESY spectrum, the NOE correlation between H-4 and H-4‴*β* was observed, suggesting the same orientation of H-4 and H-4‴*β* (Figure 3). Based on the aforementioned spectroscopic evidence, the relative configurations of three chiral centers (C-4, C-5, and C-5‴) in **1** were

https://dx.doi.org/10.1021/acsomega.0c01019
ACS Omega 2020, 5, 10167−10175

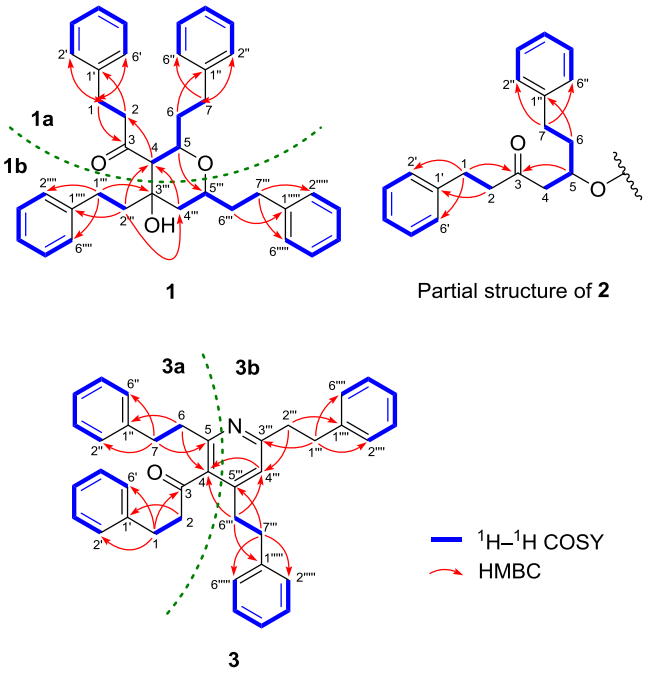

Figure 2. Key ^{1}H–^{1}H COSY and HMBC correlations of **1**–**3**.

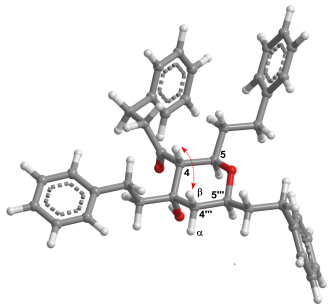

Figure 3. Geometry of the lowest energy conformer and key NOESY correlation of **1**.

assumed as 4*R**, 5*R**, and 5‴*S**, respectively. However, due to the absence of the critical NOE correlation, the relative configuration of C-3‴ in compound **1** remained unresolved. Subsequently, theoretical calculations of ^{1}H and ^{13}C NMR chemical shifts of the two plausible relative configurations of **1**, 4*R**, 5*R**, 3‴*S**, 5‴*S**-**1**, and 4*R**, 5*R**, 3‴*R**, 5‴*S**-**1** were performed with the Gaussian 09 software using the gauge-invariant atomic orbital (GIAO) method at the mPW1PW91/6-311+G(d,p) level. After comparison of the experimental NMR spectral data and the calculated ^{1}H and ^{13}C chemical shifts values, the relative configuration of **1** was determined to be 4*R**, 5*R**, 3‴*S**, 5‴*S**, of which the DP4+ probabilities of ^{1}H and ^{13}C NMR spectral data were 100 and 99.96%, respectively (Figure 4).

The optical rotation (OR) value and electronic circular dichroism (ECD) curve of **1** were barely measurable, suggesting that it was likely a racemic mixture. Indeed, further chiral resolution of **1** on a chiral phase high-performance liquid chromatography (HPLC) column led to the separation of a pair of enantiomers, (+)-**1** and (−)-**1**, in a ratio of 1:1 (Figure S31, see the Supporting Information). The mirror image of the experimental ECD spectra of (+)-**1** and (−)-**1** confirmed their enantiomeric relationship. Subsequently, the absolute configurations of (+)-**1** and (−)-**1** were determined by comparison of their experimental spectra and estimated ECD curves employing the time-dependent density functional theory (TDDFT) method. The calculated ECD curves of 4*S*, 5*S*, 3‴*R*, 5‴*R*-**1** and 4*R*, 5*R*, 3‴*S*, 5‴*S*-**1** revealed good accordance with the measured spectra of (+)-**1** and (−)-**1**, respectively (Figure 5A). Therefore, the absolute configurations of (+)-**1** and (−)-**1** were defined, as shown in Figure 1.

Alpinidinoid B (**2**) was isolated as a yellow oil with an optical rotation value of $[\alpha]_D^{20}$ + 24 (*c* 0.15, MeOH). The molecular formula of **2** was identified as $C_{38}H_{42}O_3$ on the basis of its HR–ESI–MS data with *m*/*z* 547.3212 $[M + H]^+$ (calcd for $C_{38}H_{43}O_3$: 547.3212). However, inconsistent with its molecular formula information, the ^{1}H and ^{13}C NMR spectra of **2** only showed the signals corresponding to 21 protons and 19 carbons, suggesting that **2** is a dimeric diarylheptanoid with a highly symmetrical structure (Table 2). Comprehensive analysis of the two-dimensional (2D) NMR data of **2** led to the establishment of a partial diarylheptanoid unit in **2** (Figure 2), which was close to a known monomeric diarylheptanoid (5*S*)-5-hydroxy-1,7-diphenyl-3-heptanone.[17] Besides, the HMBC correlation between H-5 (H-5‴) and C-5‴ (C-5) was observed. Considering the obvious down-field shift of C-5 (C-5‴, δ_C 72.4), along with the molecular formula information, the gross structure of **2** could be determined to be a symmetrical diarylheptanoid dimer, in which the two monomeric units were linked through C-5–*O*–C-5‴ bonds.

Due to the obvious positive specific rotation and measurable ECD Cotton effects, we could exclude the possibility that compound **2** was a mesomer. Therefore, the above-mentioned evidence demonstrated the presence of a C_2 symmetry axis in the molecule of **2**, and the following chiral HPLC analysis indicated that **2** was obtained as an optically pure compound. To further clarify the absolute configuration of **2**, quantum chemical calculation of ECD curves of two possible stereoisomers of **2**, (5*S*,5‴*S*)-**2** and (5*R*,5‴*R*)-**2**, were subsequently performed by utilizing the TDDFT method. Excellent agreement was found between the theoretical ECD curve for (5*S*,5‴*S*)-**2** and the experimental one of **2** (Figure 5B). Thus, the absolute configuration of **2** was determined to be 5*S*,5‴*S* (Figure 1).

The HR–ESI–MS data of **3** showed a protonated molecular ion peak at *m*/*z* 524.2936 $[M + H]^+$ (calcd for $C_{38}H_{38}NO$ 524.2953), which was consistent with the molecular formula of $C_{38}H_{37}NO$. The UV spectrum of **3** exhibited absorption maxima at 208 and 269 nm. The IR spectrum suggested the existence of the carbonyl group (1695 cm^{-1}) and aromatic ring (1590 and 1449 cm^{-1}) in **3**. Similar to **1**, the ^{1}H and ^{13}C NMR spectra of **3** revealed the presence of characteristic signals corresponding to two diarylheptanoid moieties, including a ketone carbonyl (δ_C 208.0), four monosubstituted benzene rings [δ_H 7.06–7.11 (4H, overlapped), 7.14–7.19 (4H, overlapped), and 7.20–7.30 (12H, overlapped); δ_C 142.7, 141.9 × 3, 129.5 × 2, 129.34 × 6, 129.27 × 2, 129.2 × 2, 129.1 × 4, 126.9, 126.8, 126.69, and 126.68], four sp^2 quaternary carbons (δ_C 161.4, 155.6, 147.2, and 135.8), one olefinic methine [δ_H 6.97 (1H, br s); δ_C 121.8], along with eight alkyl methylene groups.

The ^{1}H–^{1}H COSY spectrum of **3** revealed the existence of seven spin-coupling systems (Figure 2). To elucidate the planar structure of **3**, the HMBC correlations were further interpreted. On the one hand, the HMBC cross-peaks between H_2-1 and C-3/C-2′ (C-6′), between H_2-2 and C-1′, between

https://dx.doi.org/10.1021/acsomega.0c01019
ACS Omega 2020, 5, 10167–10175

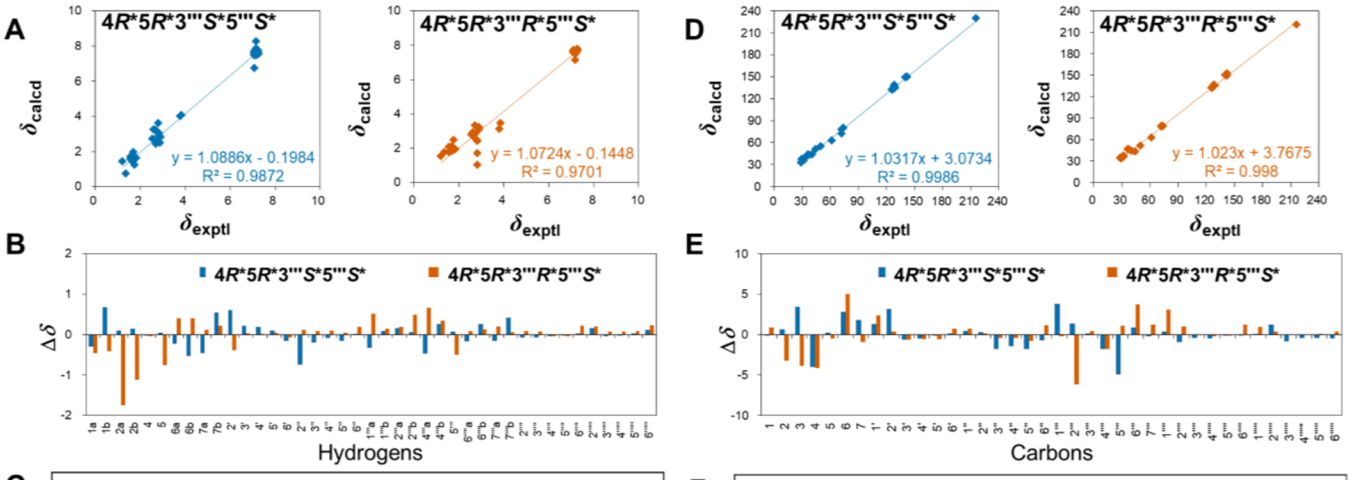

C

DP4+ probability of ^{1}H NMR of 1		
Plausible epimers	4*R**,5*R**,3'''*S**,5'''*S**	4*R**,5*R**,3'''*R**,5'''*S**
sDP4+	100%	0.00%
uDP4+	98.70%	1.30%
DP4+	100%	0.00%

F

DP4+ probability of ^{13}C NMR of 1		
Plausible epimers	4*R**,5*R**,3'''*S**,5'''*S**	4*R**,5*R**,3'''*R**,5'''*S**
sDP4+	99.04%	0.96%
uDP4+	96.31%	3.69%
DP4+	99.96%	0.04%

Figure 4. ^{1}H and ^{13}C chemical shift value calculation results of two possible stereoisomers of **1**. Linear correlation plots of the calculated vs experimental ^{1}H (^{13}C) chemical shift values for each plausible configuration of **1** (A, D). Relative errors between the calculated ^{1}H (^{13}C) chemical shift values of two plausible stereoisomers and experimental ^{1}H (^{13}C) NMR data of **1** (B, E). The DP4+ probabilities of the ^{1}H (^{13}C) NMR chemical shifts of **1** (C, F).

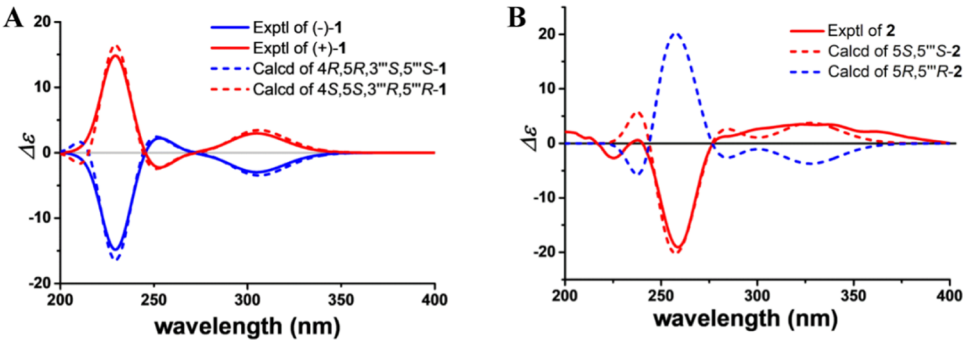

Figure 5. Calculated and experimental ECD spectra of (+)-**1** (A), (−)-**1** (A), and **2** (B).

H_2-6 and C-4/C-1″, and between H_2-7 and C-5/C-2″ (C-6″) resulted in the formation of a diarylheptanoid moiety, as shown in Figure 2 (**3a**). On the other hand, the HMBC correlations between H_2-1‴ and C-3‴/C-2‴′ (C-6‴′), between H_2-2‴ and C-1‴′/C-4‴, between H_2-6‴ and C-4‴/C-1‴″, and between H_2-7‴ and C-5‴/C-2‴″ (C-6‴″) allowed the assignment of the second diarylheptanoid moiety **3b** (Figure 2). Furthermore, the HMBC correlations between H-6‴ and C-4 and between H-4‴ and C-4, combined with the molecular formula information, indicated that the two diarylheptanoid motifs **3a** and **3b** were connected via C-4−C-5‴ and C-5−*N*−C-3‴ bonds to form an additional pyridine ring (Figure 2). Structurally, the two diarylheptanoid monomers of **3** were connected via a pyridine ring, which is very rare in naturally occurring dimeric diarylheptanoids. So far, only two analogues, officinaruminane A and officinine B, have been reported.[19,31] When we searched the structure of **3** through SciFinder Scholar, we found that this compound has been registered as a synthetic chemical with a CAS registry number of 2181082-48-2. However, this is the first report that this compound was obtained from a natural source. Therefore, we gave a trivial name alpinidinoid C for this new natural product.

(+)-1 Protects Cortical Neurons against OGD/R-Induced Damage. To test the nontoxic dosages of these compounds, cortical neurons were treated with compounds at different concentrations (1−10 μM) for 24 h, and cell viability was examined by the (3-(4,5-dimethylthiazol-2-yl)-2,5-diphenyltetrazolium bromide (MTT) assay. We found that (+)-**1** and (−)-**1** were not toxic at concentrations up to 5 μM, whereas compounds **2** and **3** had toxicity at concentrations larger than 1 μM (Figure 6A). To examine neuroprotective activities of these compounds, cortical neurons were pretreated with compounds for 4 h before OGD/R and then cell viability was measured. Compared to the control group, OGD/R reduced cell survival by 30% (Figure 6B). However, the decreased cell viability was significantly reversed by treatment with (+)-**1** (Figure 6B). These results suggest that pretreatment with (+)-**1** protects cortical neurons from OGD/R-induced damage, but compounds (−)-**1**, **2**, and **3** do not have this effect.

(+)-1 Reduces OGD/R-Induced Cell Apoptosis. To examine apoptosis after OGD/R and to determine whether (+)-**1** could inhibit apoptosis following OGD/R, we tested the apoptosis rate of cortical neurons with flow cytometry. The

https://dx.doi.org/10.1021/acsomega.0c01019
ACS Omega 2020, 5, 10167−10175

Table 2. ^{1}H and ^{13}C NMR Spectroscopic Data for 2 (in $CDCl_3$, δ in ppm, J in Hz)[a]

no.	δ_C	δ_H
1/1‴	29.5	2.89 (t, 7.5)
2/2‴	45.5	a: 2.78 (dt, 17.5, 7.5)
		b: 2.72
3/3‴	208.7	
4/4‴	47.4	a: 2.71 (dd, 16.4, 6.7)
		b: 2.34 (dd, 16.4, 5.2)
5/5‴	72.4	3.88 (m)
6/6‴	36.2	1.75 (m)
7/7‴	31.5	2.61 (m)
1′/1‴′	141.0	
2′/2‴′, 6′/6‴′	128.3[b]	7.16−7.20
3′/3‴′, 5′/5‴′	128.4[b]	7.26−7.29
4′/4‴′	126.1	7.16−7.20
1″/1‴″	141.8	
2″/2‴″, 6″/6‴″	128.4[b]	7.14
3″/3‴″, 5″/5‴″	128.5[b]	7.26−7.29
4″/4‴″	125.9	7.16−7.20

[a]Overlapped resonances are reported without designating multiplicity. [b]Interchangeable assignments.

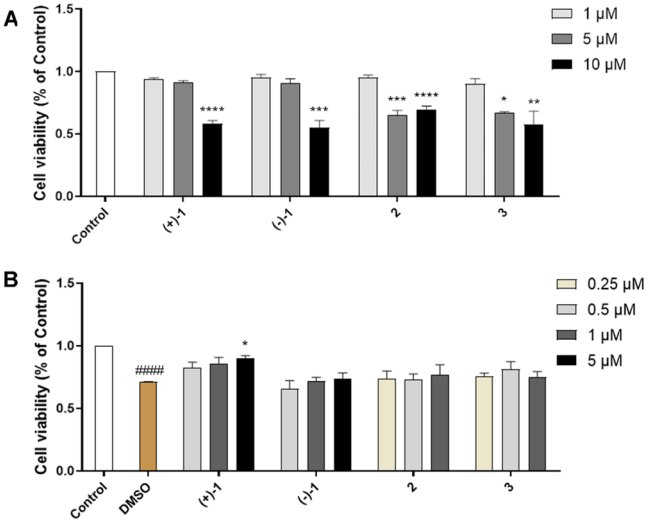

Figure 6. (+)-1 protects cortical neurons against OGD/R-induced cell damage. (A) Cytotoxicity was measured by the MTT assay. *p < 0.05, **p < 0.01, ***p < 0.001, ****p < 0.0001 vs control. (B) Cell viability was measured by the MTT assay. ####p < 0.0001 vs control. *p < 0.05 vs dimethyl sulfoxide (DMSO) group. The data represent the mean ± standard error of mean (SEM) of three independent experiments.

results showed that compared with the DMSO treatment group, (+)-1 pretreatment significantly decreased neuronal apoptosis following OGD/R, suggesting that (+)-1 protects cortical neurons against OGD/R-induced apoptosis (Figure 7A,B).

(+)-1 Inhibits the Expression of Cleaved-Caspase-3 and Upregulates the AKT/mTOR Signaling Pathway during OGD/R. Subsequently, we explored whether the level of cleaved-caspase-3, an important apoptosis-related protein, is regulated by (+)-1. Cortical neurons pretreated with (+)-1 for 4 h were subjected to OGD/R, and cleaved-caspase-3 was detected in neuron homogenates by western blotting. According to the results in Figure 8A,B, OGD/R increased

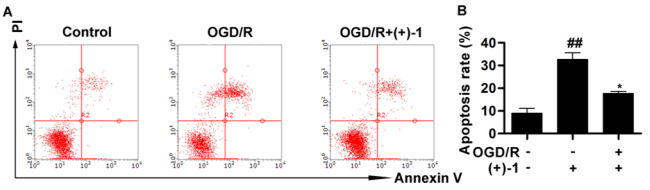

Figure 7. (+)-1 inhibits OGD/R-induced neuronal apoptosis. (A) Cortical neurons were pretreated with 5 μM (+)-1 for 4 h followed by 4 h OGD and 24 h reoxygenation. Apoptosis neurons were detected with Annexin V/PI staining by flow cytometry. (B) Apoptosis rate of cortical neurons measured by flow cytometry. ##p < 0.01, vs Control. *p < 0.01, vs OGD/R group. The data represent the mean ± SEM of three independent experiments.

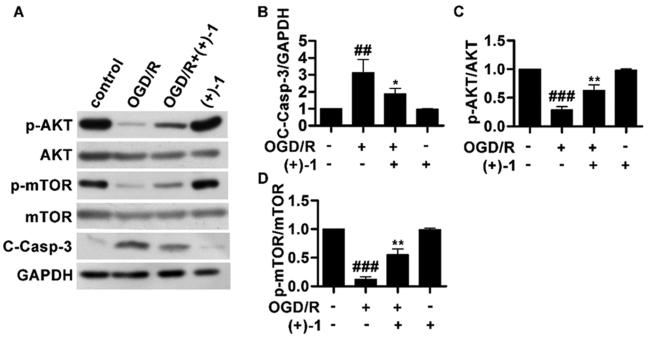

Figure 8. (+)-1 reverses OGD/R-induced upregulation of cleaved-caspase-3 and downregulation of the AKT/mTOR signaling pathway in cortical neurons. (A) Levels of phosphorylated p-AKT, p-mTOR, and cleaved-caspase-3 (C-Casp-3) in OGD/R-damaged neurons are reversed by (+)-1 pretreatment. (B−D) Relative band density of C-Casp-3 (B), p-AKT (C), and p-mTOR (D) were measured with ImageJ and normalized to that of GAPDH. ##p < 0.01, ###p < 0.001, vs Control. *p < 0.05, **p < 0.01, ***p < 0.001, vs OGD/R group. Data are presented as mean ± SEM from at least three independent experiments.

the level of cleaved-caspase-3, which was significantly downregulated in the OGD/R group treated with (+)-1. The AKT/mTOR signaling pathway plays an essential role in inhibiting apoptosis. To explore the neuroprotective molecular mechanism of (+)-1, we examined the phosphorylation levels of AKT and mTOR, which reflect the active states of the two proteins. We found that OGD/R markedly inhibited the phosphorylation of AKT and mTOR, which could be reversed by (+)-1 pretreatment (Figure 8A−D). By contrast, (−)-1 had no effects on either cleaved-caspase-3 or AKT/mTOR phosphorylation. These results indicate that the AKT/mTOR signaling pathway could be involved in the (+)-1-mediated neuroprotective effect in OGD/R-exposed cortical neurons.

Neuroprotective Effect of (+)-1 is Mediated through the PI3K/AKT/mTOR Signaling Pathway. To verify whether the PI3K/AKT/mTOR pathway is critical in (+)-1-mediated neuronal protection, we examined whether the PI3K-specific inhibitor LY294002 (10 μM) and the mTOR inhibitor Torin1 (30 nM) affect the activity of (+)-1. The ERK inhibitor U0126 (10 μM) was also examined as a control. Indeed, western blotting results revealed that LY294002 and Torin1 canceled the effect of (+)-1 on cleaved-caspase-3 inhibition after OGD/R (Figure 9A,B). Consistently, the cell viability assay also confirmed that LY294002 and Torin1 abrogated the neuroprotection effect of (+)-1 (Figure 9C). By contrast, U0126 exerted no interfering actions on (+)-1, suggesting that

https://dx.doi.org/10.1021/acsomega.0c01019
ACS Omega 2020, 5, 10167−10175

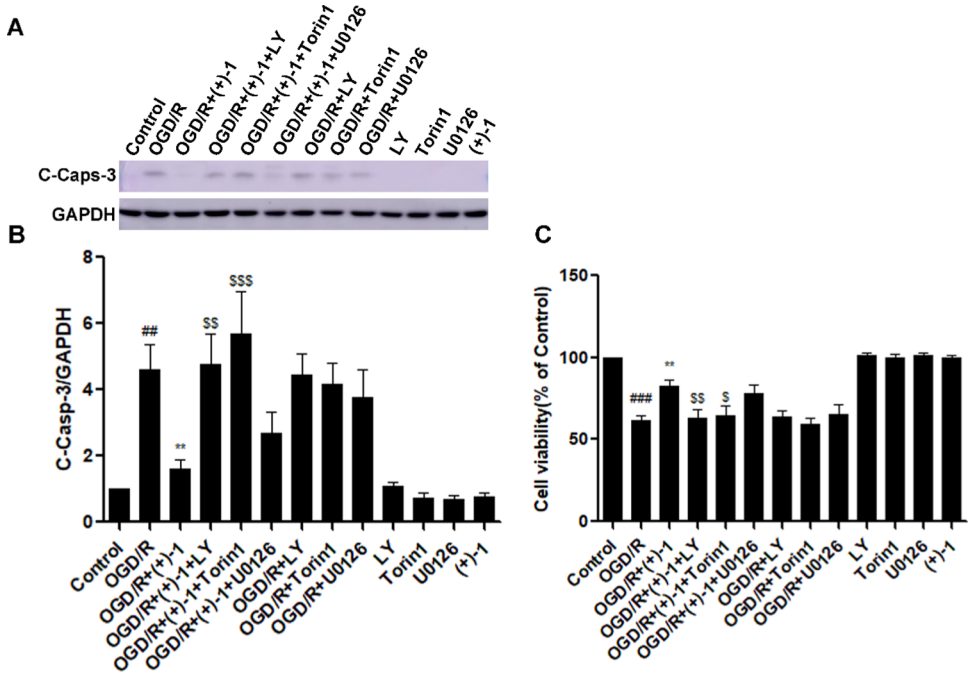

Figure 9. (+)-**1** protects OGD/R-induced cortical neuronal injury through the PI3K/AKT/mTOR signaling pathway. (A) Treatment of LY294002 (LY) and Torin1 blocked the effect of (+)-**1** to attenuate the expression levels of C-Casp-3 in OGD/R-damaged neurons. (B) Relative band density of C-Casp-3 was measured with ImageJ and normalized to that of GAPDH. $^{\#\#}p < 0.01$, vs control. $^{**}p < 0.01$, vs OGD/R group. $^{\$\$}p < 0.01$, $^{\$\$\$}p < 0.001$, vs OGD/R+ (+)-**1** group. (C) Cell viability was measured by MTT. $^{\#\#\#}p < 0.001$, vs control. $^{**}p < 0.01$, vs OGD/R group. $^{\$}p < 0.05$, $^{\$\$}p < 0.01$, vs OGD/R+ (+)-**1** group. Data are presented as mean ± SEM from at least three independent experiments.

ERK does not participate in the function of (+)-**1**. Therefore, (+)-**1** has a protective effect in cortical neurons against OGD/R through the PI3K/AKT/mTOR signaling pathway.

CONCLUSIONS

In conclusion, the phytochemical investigation of the petroleum ether-soluble fraction of *A. officinarum* resulted in the isolation and identification of three dimeric diarylheptanoids, including a pair of new dimeric diarylheptanoid enantiomers [(±)-alpinidinoid A, (±)-**1**] and a new axisymmetrical diarylheptanoid dimer (alpinidinoid B, **2**) possessing two unusual connecting manners, and a new naturally occurring dimeric diarylheptanoid with a rare pyridine ring linkage (alpinidinoid C, **3**). Among them, (+)-**1** exhibits protective effects against OGD/R-induced primary cortical neurons apoptosis. Moreover, (+)-**1** significantly decreased the expression of cleaved-caspase-3. The protective effect of (+)-**1** is achieved via activating the PI3K/AKT/mTOR signaling pathway. Therefore, this dimeric diarylheptanoid from the widely used *A. officinarum* holds beneficial potential to be used as a candidate agent for treating cerebral ischemic injury.

MATERIALS AND METHODS

General Experimental Procedures. Details on instruments for structural elucidation (UV, IR, optical rotations, ECD, NMR, HR−ESI−MS), along with the materials for isolation (silica gel, octadecyl silica, liquid chromatograph system, and solvents), have been described in our previous work.[23]

Plant Material. The rhizomes of *A. officinarum* Hance (Zingiberaceae) were cultivated and collected from Longtang Town, Xuwen County, Guangdong Province of People's Republic of China, in December 2013. The plant material was identified by Prof. Guang-Xiong Zhou (Institute of Traditional Chinese Medicine & Natural Products, Jinan University), and a voucher specimen (No. 20131211) has been stored in the Institute of Traditional Chinese Medicine & Natural Products, College of Pharmacy, Jinan University, Guangzhou.

Extraction and Isolation. The general extraction and partition procedures of the rhizomes of *A. officinarum* were described in our previous report.[23] In this work, the petroleum ether-soluble fraction (500 g) was subjected to a silica gel column using a gradient mixture of petroleum ether and EtOAc (1:0 → 2:1, v/v) as eluent to afford 12 major fractions (1−12). Fraction 3 (56 g) was separated on a silica gel column with a cyclohexane−EtOAc mixture (1:0 → 0:1, v/v) as eluent to obtain seven subfractions (3A−3G). Subfraction 3C (6.4 g) was subjected to an ODS column eluted with a gradient mixture of MeOH and H_2O (30:70 → 100:0, v/v) to afford five subfractions (3C-1−3C-5). Subfraction 3C-3 (1.5 g) was further separated by a Sephadex LH-20 column ($CHCl_3$−MeOH, 50:50, v/v) and subsequently purified by reversed-phase preparative HPLC using MeOH−H_2O (90:10, v/v, 6 mL/min) as the mobile phase to yield compound **1** (6.8 mg). Fraction 4 (61 g) was subjected to a silica gel column eluted with a gradient mixture of petroleum ether and EtOAc (100:5 → 1:1, v/v) to afford five subfractions (4A−4E). Subfraction 4B (7.6 g) was then separated on an ODS column with MeOH−H_2O (20:80 → 90:10, v/v) as eluent to yield five subfractions (4B-1−4B-5). Subfraction 4B-2 (1.1 g) was subsequently purified by reversed-phase preparative HPLC, using CH_3CN−H_2O (75:25, v/v, 6 mL/min) as the mobile phase to afford compound **2** (4.8 mg). Compound **3** (4.5 mg) was afforded from subfraction 4B-3 (0.75 g) by preparative HPLC using CH_3CN−H_2O (80:20, v/v, 6 mL/min) as the mobile phase.

https://dx.doi.org/10.1021/acsomega.0c01019
ACS Omega 2020, 5, 10167−10175

Chiral Resolution of Enantiomers. Chiral resolution of (±)-**1** was carried out on an Agilent 1260 liquid chromatograph system equipped with a DAD detector and a Phenomenex Cellulose-4 column (4.6 mm × 250 mm, i.d. 5 μm, Phenomenex, CA). A pair of enantiomers (+)-**1** (t_R 11.9 min, 1.6 mg) and (−)-**1** (t_R 12.4 min, 1.5 mg) were obtained, respectively, by employing MeOH−H_2O (80:20, v/v) as the mobile phase, with a flow rate of 1 mL/min.

*(±)-Alpinidinoid A (**1**).* Yellow oil; $[\alpha]_{25}^{D}$ ± 0 (*c* 0.1, MeOH); UV (MeOH) λ_{max} (log ε) 208 (3.43), 262 (1.89) nm; IR (KBr) ν_{max} 3448, 2928, 1687, 1633, 1601, 1493, 1454, 1385, 1117, 1063, 746, 699 cm^{-1}; ^1H NMR ($CDCl_3$, 500 MHz) and ^{13}C NMR ($CDCl_3$, 125 MHz) data, see Table 1; HR−ESI−MS *m*/*z* 545.3055 $[M - H]^-$ (calcd for $C_{38}H_{41}O_3$, 545.3056).

(+)-**1**: yellow oil; $[\alpha]_{25}^{D}$ + 28 (*c* 0.16, MeOH); ECD (MeOH, Δε) λ_{max} 229 (+14.83), 253 (−2.24), 305 (+2.96) nm.

(−)-**1**: yellow oil; $[\alpha]_{25}^{D}$ − 28 (*c* 0.15, MeOH); ECD (MeOH, Δε) λ_{max} 229 (−14.83), 253 (+2.24), 305 (−2.96) nm.

*Alpinidinoid B (**2**).* Yellow oil; $[\alpha]_{25}^{D}$ +24 (*c* 0.15, MeOH); UV (MeOH) λ_{max} (log ε) 209 (3.66), 260 (2.09) nm; IR (KBr) ν_{max} 2923, 1711, 1645, 1601, 1495, 1449, 1365, 1069, 746, 700, 481 cm^{-1}; ECD (MeOH, Δε) λ_{max} 259 (−19.05), 322 (+3.48) nm; ^1H NMR ($CDCl_3$, 600 Hz) and ^{13}C NMR ($CDCl_3$, 150 MHz) data, see Table 2; HR−ESI−MS *m*/*z* 547.3212 $[M + H]^+$ (calcd for $C_{38}H_{43}O_3$, 547.3212).

*Alpinidinoid C (**3**).* Yellow oil; UV (MeOH) λ_{max} (log ε) 208 (3.59), 269 (2.58) nm; IR (KBr) ν_{max} 3447, 2928, 1695, 1631, 1590, 1552, 1449, 1387, 1076, 1028, 746, 700 cm^{-1}; ^1H NMR (acetone-d_6, 500 MHz) and ^{13}C NMR (acetone-d_6, 125 MHz) data, see Table 1; HR−ESI−MS *m*/*z* 524.2936 $[M + H]^+$ (calcd for $C_{38}H_{38}NO$, 524.2953).

Computational Methods. The Gaussian 09 program package was employed to perform the calculation.[26] The general computational methods for conformational analysis, energy optimization, and NMR and ECD simulation were similar to those in our previous report.[23] Differently, the NMR data of all the selected conformers were calculated with the GIAO/mPW1PW91/6-311+G(d,p) methods in the gas phase. Also, the overall simulated CD curves were generated by the Boltzmann distribution of each conformer using SpecDis 1.71 software,[27] and the theoretical NMR data were analyzed by using linear regression and DP4+ probability.[28]

Culture of Primary Cortical Neurons. Primary cortical neurons were prepared from E18 Sprague−Dawley rat embryos as previously described.[29,30] Briefly, cortical neurons were dissociated for 15 min at 37 °C in 5 mL of calcium and magnesium-free Hank's balanced salt solution (CMF-HBSS) (Life Technologies, CA) with 0.05% trypsin. Then, cells were centrifuged at 1000 rpm for 5 min, and the neurons were resuspended with Neurobasal medium (Life Technologies, CA) supplemented with 2% B27 (Life Technologies, CA). Cortical cells were seeded onto 96-well plates (1×10^5 per well) precoated with poly-L-lysine (Sigma-Aldrich, St. Louis, MO) for the MTT assay, and 35 mm dishes (8×10^5 per dish) for western blot analysis. The neurons were cultured for 7 days (7 days in vitro; DIV) for experiments.

Oxygen-Glucose Deprivation and Reoxygenation (OGD/R) Model and Compound Treatment. Neurons were randomly divided into control group, OGD/R group, and OGD/R+ (+)-**1** group. Cortical neurons were pretreated with 5 μM (+)-**1** for 4 h in a normal medium. Then, the culture media were changed into glucose-free Dulbecco's modified Eagle's medium (DMEM) (Life Technologies) and the cortical neurons were placed in a Modular Incubator Chamber (MIC-101) (Billups-rothenberg, Inc.) filled with a mixed gas of 95% N_2 and 5% CO_2 for 4 h. Afterwards, reoxygenation was simulated by replacing the glucose-free medium with a normal culture medium for 24 h. Control cells were not exposed to OGD/R. Cell survival was determined by the MTT assay.

Measurement of Cell Viability. Cell viability was performed by the MTT assay.[21,25] Briefly, the culture medium was removed and MTT (5 mg/mL) was added to cells for 4 h, and then MTT was replaced with DMSO to dissolve formazan. The solution was centrifuged for 3 min at 3000 rpm. The absorbance values were detected at 595 nm in a microplate reader (Beckman coulter). Cell viability was presented as a percentage of the control group.

Detection of Apoptosis Using Flow Cytometry. Briefly, primary cortical neurons were collected by centrifugation, washed twice using cold phosphate buffered saline (PBS) buffer, and resuspended with 1× Annexin-binding buffer. Next, cells were incubated with Annexin V-FITC and PI for 15 min at room temperature in the dark. Finally, the antiapoptosis effect was measured by flow cytometry according to the manufacturer's instructions (Abcam, U.K.).

Western Blot Analysis. At DIV 7, cells were pretreated with (+)-**1** for 4 h and were insulted with OGD/R in glucose-free DMEM (Life Technologies). The cells were washed twice with cold PBS, collected in the radioimmunoprecipitation assay (RIPA) buffer accompanied with a protease inhibitor (Bimake), and lysed on ice for 30 min. Cell lysis was centrifuged at 4 °C, 12 000 rpm for 15 min. The protein concentration in the supernatant was determined with a BCA assay kit (Beyotime Biotechnology, China). The sodium dodecyl sulfate (SDS) sample buffer was added for denaturing the proteins, which were separated by 8−12% SDS-polyacrylamide gel electrophoresis (PAGE). The anti-rabbit primary antibodies used in Western Blot Analysis were p-AKT (1:1000, Cell Signaling Technology), AKT (1:1000, Cell Signaling Technology), p-mTOR (1:1000, Cell Signaling Technology), mTOR (1:1000, Cell Signaling Technology), cleased-caspase-3 (1:1000, Cell Signaling Technology), or GAPDH (1:5000, Abbkine).

Statistical Analysis. Data processing and analysis were performed by using GraphPad Prism 5 software. All data were expressed as means ± standard error of mean (SEM) of at least three independent experiments. The difference between groups was assessed using one-way analysis of variance (ANOVA) followed by Bonferroni's multiple comparison test.

■ ASSOCIATED CONTENT

Supporting Information

The Supporting Information is available free of charge at https://pubs.acs.org/doi/10.1021/acsomega.0c01019.

HR−ESI−MS, UV, IR, one-dimensional (1D), and 2D NMR spectra of compounds **1**−**3**, chiral HPLC separation of compound **1**, as well as NMR and ECD computational details of compounds **1** and **2** (PDF)

https://dx.doi.org/10.1021/acsomega.0c01019
ACS Omega 2020, 5, 10167−10175

AUTHOR INFORMATION

Corresponding Authors

Ying Wang − *Institute of Traditional Chinese Medicine & Natural Products, JNU-HKUST Joint Laboratory for Neuroscience & Innovative Drug Research, and Guangdong Province Key Laboratory of Pharmacodynamic Constituents of TCM & New Drugs Research, Jinan University, Guangzhou 510632, People's Republic of China;* orcid.org/0000-0003-4524-1812; Email: wangying_cpu@163.com

Lei Shi − *JNU-HKUST Joint Laboratory for Neuroscience & Innovative Drug Research and Guangdong Province Key Laboratory of Pharmacodynamic Constituents of TCM & New Drugs Research, Jinan University, Guangzhou 510632, People's Republic of China;* orcid.org/0000-0001-8695-3432; Email: sophielshi80@gmail.com, t_shilei@jnu.edu.cn

Authors

Hui Liu − *Institute of Traditional Chinese Medicine & Natural Products, JNU-HKUST Joint Laboratory for Neuroscience & Innovative Drug Research, and Guangdong Province Key Laboratory of Pharmacodynamic Constituents of TCM & New Drugs Research, Jinan University, Guangzhou 510632, People's Republic of China*

Xiaojun Wang − *JNU-HKUST Joint Laboratory for Neuroscience & Innovative Drug Research and Guangdong Province Key Laboratory of Pharmacodynamic Constituents of TCM & New Drugs Research, Jinan University, Guangzhou 510632, People's Republic of China;* orcid.org/0000-0002-7117-1363

Qiaoyun Shi − *JNU-HKUST Joint Laboratory for Neuroscience & Innovative Drug Research and Guangdong Province Key Laboratory of Pharmacodynamic Constituents of TCM & New Drugs Research, Jinan University, Guangzhou 510632, People's Republic of China*

Liuren Li − *JNU-HKUST Joint Laboratory for Neuroscience & Innovative Drug Research and Guangdong Province Key Laboratory of Pharmacodynamic Constituents of TCM & New Drugs Research, Jinan University, Guangzhou 510632, People's Republic of China*

Qinghua Zhang − *JNU-HKUST Joint Laboratory for Neuroscience & Innovative Drug Research and Guangdong Province Key Laboratory of Pharmacodynamic Constituents of TCM & New Drugs Research, Jinan University, Guangzhou 510632, People's Republic of China*

Zhen-Long Wu − *Institute of Traditional Chinese Medicine & Natural Products, JNU-HKUST Joint Laboratory for Neuroscience & Innovative Drug Research, and Guangdong Province Key Laboratory of Pharmacodynamic Constituents of TCM & New Drugs Research, Jinan University, Guangzhou 510632, People's Republic of China;* orcid.org/0000-0001-8985-7980

Xiao-Jun Huang − *Institute of Traditional Chinese Medicine & Natural Products, JNU-HKUST Joint Laboratory for Neuroscience & Innovative Drug Research, and Guangdong Province Key Laboratory of Pharmacodynamic Constituents of TCM & New Drugs Research, Jinan University, Guangzhou 510632, People's Republic of China;* orcid.org/0000-0002-3636-4813

Qing-Wen Zhang − *State Key Laboratory of Quality Research in Chinese Medicine, Institute of Chinese Medical Sciences, University of Macau, Macao 999078, People's Republic of China*

Wen-Cai Ye − *Institute of Traditional Chinese Medicine & Natural Products, JNU-HKUST Joint Laboratory for Neuroscience & Innovative Drug Research, and Guangdong Province Key Laboratory of Pharmacodynamic Constituents of TCM & New Drugs Research, Jinan University, Guangzhou 510632, People's Republic of China;* orcid.org/0000-0002-2810-1001

Complete contact information is available at: https://pubs.acs.org/10.1021/acsomega.0c01019

Author Contributions

⊥H.L., X.W., and Q.S. contributed equally to this work.

Funding

This work was supported by the Academy of Medical Sciences Newton Advanced Fellowship in partnership with The Royal Society and the National Natural Science Foundation of China [UK/China grant numbers: AOMS-NAF0051003/81761130084], the Science & Technology Program of China (2019ZX09735002), the National Natural Science Foundation of China (81630095 and 81803379), the Key Realm R&D Program of Guangdong Province (2019B030335001), and the Local Innovative and Research Teams Project of Guangdong Pearl River Talents Program (2017BT01Y036).

Notes

The authors declare no competing financial interest.

ACKNOWLEDGMENTS

We acknowledge Jinan University, Guangzhou, China, for allowing us to use their high-performance computing platform for computation.

REFERENCES

(1) Flynn, R. W.; MacWalter, R. S.; Doney, A. S. The cost of cerebral ischaemia. *Neuropharmacology* **2008**, *55*, 250−256.

(2) Raichle, M. E. The pathophysiology of brain ischemia. *Ann. Neurol.* **1983**, *13*, 2−10.

(3) Benjamin, E. J.; Muntner, P.; Alonso, A.; Bittencourt, M. S.; Callaway, C. W.; Carson, A. P.; Chamberlain, A. M.; Chang, A. R.; Cheng, S.; Das, S. R.; Delling, F. N.; Djousse, L.; Elkind, M. S. V.; Ferguson, J. F.; Fornage, M.; Jordan, L. C.; Khan, S. S.; Kissela, B. M.; Knutson, K. L.; Kwan, T. W.; Lackland, D. T.; Lewis, T. T.; Lichtman, J. H.; Longenecker, C. T.; Loop, M. S.; Lutsey, P. L.; Martin, S. S.; Matsushita, K.; Moran, A. E.; Mussolino, M. E.; O'Flaherty, M.; Pandey, A.; Perak, A. M.; Rosamond, W. D.; Roth, G. A.; Sampson, U. K. A.; Satou, G. M.; Schroeder, E. B.; Shah, S. H.; Spartano, N. L.; Stokes, A.; Tirschwell, D. L.; Tsao, C. W.; Turakhia, M. P.; VanWagner, L. B.; Wilkins, J. T.; Wong, S. S.; Virani, S. S.; American Heart Association Council on, Epidemiology and Prevention Statistics Committee and Stroke Statistics Subcommittee. Heart Disease and Stroke Statistics-2019 Update: A Report From the American Heart Association. *Circulation* **2019**, *139*, e56−e528.

(4) Tobin, M. K.; Bonds, J. A.; Minshall, R. D.; Pelligrino, D. A.; Testai, F. D.; Lazarov, O. Neurogenesis and inflammation after ischemic stroke: what is known and where we go from here. *J. Cereb. Blood Flow Metab.* **2014**, *34*, 1573−1584.

(5) Papanagiotou, P.; White, C. J. Endovascular Reperfusion Strategies for Acute Stroke. *JACC: Cardiovasc. Interventions* **2016**, *9*, 307−317.

(6) Lo, E. H.; Dalkara, T.; Moskowitz, M. A. Mechanisms, challenges and opportunities in stroke. *Nat. Rev. Neurosci.* **2003**, *4*, 399−415.

(7) Broughton, B. R. S.; Reutens, D. C.; Sobey, C. G. Apoptotic mechanisms after cerebral ischemia. *Stroke* **2009**, *40*, e331−e339.

(8) Wouters, B. G.; Koritzinsky, M. Hypoxia signalling through mTOR and the unfolded protein response in cancer. *Nat. Rev. Cancer* **2008**, *8*, 851−864.
(9) Yan, H.; Zhang, X.; Hu, W.; Ma, J.; Hou, W.; Zhang, X.; Wang, X.; Gao, J.; Shen, Y.; Lv, J.; Ohtsu, H.; Han, F.; Wang, G.; Chen, Z. Histamine H3 receptors aggravate cerebral ischaemic injury by histamine-independent mechanisms. *Nat. Commun.* **2014**, *5*, No. 3334.
(10) Yang, Z.; Weian, C.; Susu, H.; Hanmin, W. Protective effects of mangiferin on cerebral ischemia-reperfusion injury and its mechanisms. *Eur. J. Pharmacol.* **2016**, *771*, 145−151.
(11) Li, L.; Xue, J.; Liu, R.; Li, X.; Lai, L.; Xie, J.; Huang, Z.; Huang, C. Neuroprotective effects of genistein-3′-sodium sulfonate on focal cerebral ischemia in rats. *Neurosci. Lett.* **2017**, *646*, 43−48.
(12) Tang, K. S.; Tan, J. S. The protective mechanisms of polydatin in cerebral ischemia. *Eur. J. Pharmacol.* **2019**, *842*, 133−138.
(13) Zhou, Y. Q.; Liu, H.; He, M. X.; Wang, R.; Zeng, Q. Q.; Wang, Y.; Ye, W. C.; Zhang, Q. W. Chapter 11—A Review of the Botany, Phytochemical, and Pharmacological Properties of Galangal. In *Natural and Artificial Flavoring Agents and Food Dyes*; Grumezescu, A. M.; Holban, A. M., Eds.; Academic Press, 2018; pp 351−396.
(14) Shin, D.; Kinoshita, K.; Koyama, K.; Takahashi, K. Antiemetic Principles of *Alpinia Officinarum*. *J. Nat. Prod.* **2002**, *65*, 1315−1318.
(15) Yang, Y.; Kinoshita, K.; Koyama, K.; Takahashi, K.; Kondo, S.; Watanabe, K. Structure-antiemetic-activity of some diarylheptanoids and their analogues. *Phytomedicine* **2002**, *9*, 146−152.
(16) Ly, T. N.; Shimoyamada, M.; Kato, K.; Yamauchi, R. Isolation and characterization of some antioxidative compounds from the rhizomes of smaller galanga (*Alpinia officinarum* Hance). *J. Agric. Food Chem.* **2003**, *51*, 4924−4929.
(17) Zhang, B.-B.; Dai, Y.; Liao, Z.-X.; Ding, L.-S. Three new antibacterial active diarylheptanoids from *Alpinia officinarum*. *Fitoterapia* **2010**, *81*, 948−952.
(18) An, N.; Zou, Z. M.; Tian, Z.; Luo, X. Z.; Yang, S. L.; Xu, L. Z. Diarylheptanoids from the rhizomes of *Alpinia officinarum* and their anticancer activity. *Fitoterapia* **2008**, *79*, 27−31.
(19) An, N.; Zhang, H. W.; Xu, L. Z.; Yang, S. L.; Zou, Z. M. New diarylheptanoids from the rhizome of *Alpinia officinarum* Hance. *Food Chem.* **2010**, *119*, 513−517.
(20) Honmore, V. S.; Kandhare, A. D.; Kadam, P. P.; Khedkar, V. M.; Sarkar, D.; Bodhankar, S. L.; Zanwar, A. A.; Rojatkar, S. R.; Natu, A. D. Isolates of *Alpinia officinarum* Hance as COX-2 inhibitors: Evidence from anti-inflammatory, antioxidant and molecular docking studies. *Int. Immunopharmacol.* **2016**, *33*, 8−17.
(21) Xiao, H.; Zhang, Q.; Peng, Y.; Tang, G.; Liao, Y.; Zhuang, X.; Ye, W.-C.; Wang, Y.; Shi, L. 7-(4-Hydroxy-3-methoxyphenyl)-1-phenyl-4E-hepten-3-one alleviates Abeta1-42 induced cytotoxicity through PI3K-mTOR pathways. *Biochem. Biophys. Res. Commun.* **2017**, *484*, 365−371.
(22) Tang, G.; Dong, X.; Huang, X.; Huang, X.-J.; Liu, H.; Wang, Y.; Ye, W.-C.; Shi, L. A natural diarylheptanoid promotes neuronal differentiation via activating ERK and PI3K-Akt dependent pathways. *Neuroscience* **2015**, *303*, 389−401.
(23) Liu, H.; Wu, Z.-L.; Huang, X.-J.; Peng, Y.; Huang, X.; Shi, L.; Wang, Y.; Ye, W.-C. Evaluation of diarylheptanoid-terpene adduct enantiomers from *Alpinia officinarum* for neuroprotective activities. *J. Nat. Prod.* **2018**, *81*, 162−170.
(24) Huang, X.; Tang, G.; Liao, Y.; Zhuang, X.; Dong, X.; Liu, H.; Huang, X.-J.; Ye, W.-C.; Wang, Y.; Shi, L. 7-(4-Hydroxyphenyl)-1-phenyl-4E-hepten-3-one, a diarylheptanoid from *Alpinia officinarum*, protects neurons against amyloid-β induced toxicity. *Biol. Pharm. Bull.* **2016**, *39*, 1961−1967.
(25) Shi, Q.; Zhang, Q.; Peng, Y.; Zhang, X.; Wang, Y.; Shi, L. A natural diarylheptanoid protects cortical neurons against oxygen-glucose deprivation-induced autophagy and apoptosis. *J. Pharm. Pharmacol.* **2019**, *71*, 1110−1118.
(26) Frisch, M. J.; Trucks, G. W.; Schlegel, H. B.; Scuseria, G. E.; Robb, M. A.; Cheeseman, J. R.; Scalmani, G.; Barone, V.; Mennucci, B.; Petersson, G. A. et al. *Gaussian 09*, revision A.02; Gaussian, Inc.: Wallingford CT, 2009.
(27) Burhn, T.; Schaumloffel, A.; Hemberger, Y.; Pescitelli, G. *SpecDis*, version 1.71; Berlin, Germany, 2017.
(28) Grimblat, N.; Zanardi, M. M.; Sarotti, A. M. Beyond DP4: an improved probability for the stereochemical assignment of isomeric compounds using quantum chemical calculations of NMR shifts. *J. Org. Chem.* **2015**, *80*, 12526−12534.
(29) Xiao, Y.; Peng, Y.; Wan, J.; Tang, G.; Chen, Y.; Tang, J.; Ye, W.-C.; Ip, N. Y.; Shi, L. The atypical guanine nucleotide exchange factor Dock4 regulates neurite differentiation through modulation of Rac1 GTPase and actin dynamics. *J. Biol. Chem.* **2013**, *288*, 20034−20045.
(30) Guo, D.; Peng, Y.; Wang, L.; Sun, X.; Wang, X.; Liang, C.; Yang, X.; Li, S.; Xu, J.; Ye, W.-C.; Jiang, B.; Shi, L. Autism-like social deficit generated by Dock4 deficiency is rescued by restoration of Rac1 activity and NMDA receptor function. *Mol. Psychiatry* **2019**, 1−15.
(31) Zhao, L.; Liang, J. Y.; Qu, W. A novel dimeric diarylheptanoid from the rhizomes of *Alpinia officinarum*. *Chem. Nat. Compd.* **2012**, *48*, 836−838.

https://dx.doi.org/10.1021/acsomega.0c01019
ACS Omega 2020, 5, 10167−10175